

# Low-lying states in near-magic odd-odd nuclei and the effective interaction

B. G. Carlsson<sup>1</sup> and J. Toivanen<sup>2</sup>

<sup>1</sup> *Division of Mathematical Physics, LTH, Lund University,  
Post Office Box 118, S-22100 Lund, Sweden\* and*

<sup>2</sup> *Department of Physics, University of Jyväskylä, P.O. Box 35 (YFL) FI-40014, Finland  
(Dated: June 3, 2014)*

The iterative quasi-particle-random-phase approximation (QRPA) method we previously developed [1–3] to accurately calculate properties of individual nuclear states is extended so that it can be applied for nuclei with odd numbers of neutrons and protons. The approach is based on the proton-neutron-QRPA (pnQRPA) and uses an iterative non-hermitian Arnoldi diagonalization method where the QRPA matrix does not have to be explicitly calculated and stored. The method is used to calculate excitation energies of proton-neutron multiplets for several nuclei. The influence of a pairing interaction in the  $T = 0$  channel is studied.

PACS numbers: 21.60.Jz, 21.10.Re

## I. INTRODUCTION

While static properties of atomic nuclei are very interesting, much can be learned by considering dynamical effects such as the linear response of nuclei when perturbed by external fields. This can be modeled using the quasiparticle-random-phase approximation (QRPA) [4] where the external field excites quasiparticle pairs. In the standard pp-nnQRPA approach the excitations are composed of sums of two-proton and two-neutron quasiparticle excitations. If the field is instead allowed to excite proton-neutron quasiparticle pairs, the corresponding approximation is denoted pnQRPA [4]. With the pnQRPA formalism one can model nuclear reactions where in the final state a proton has turned into a neutron or vice versa as occurs in the  $\beta$ -decay processes. However, when modeling  $\beta$ -decay using nuclear density-functional theory (DFT), the results are sensitive to the effective isoscalar pairing interaction used in the model. Therefore, in recent studies of  $\beta$ -decay, the isoscalar pairing interaction is often used as a free fitting parameter [5, 6]. In order to develop better effective interactions one may try to find an optimal value for the isoscalar pairing strength without directly fitting it to the  $\beta$ -decay probabilities. The challenge in this respect is that this part of the interaction does not play a role in standard Hartree-Fock-Bogoliubov (HFB) calculations where pairing between protons and neutrons are not allowed. Therefore whatever value is employed does not influence HFB calculations for the ground state.

In a series of papers [1–3, 7] we have developed fast and memory efficient QRPA solvers which can easily be used for fine tuning model parameters while taking dynamical effects into account. In this work we extend these methods to the pnQRPA case and apply the approach to find the strength of the isoscalar pairing interaction. A value of the strength is found by using the pnQRPA to calculate

the low-lying spectra of odd-odd nuclei. Starting from a spherical nucleus and exciting a proton-neutron pair, the particles can couple their angular momenta forming a multiplet of final angular momentum values. Without any residual interaction the states of the multiplet become degenerate but in general they will split apart. The splitting between such multiplet states was very early interpreted using empirical rules [8] which stated that the nucleons prefer to align their intrinsic spins in parallel as in the case of deuterium. Using a delta interaction the gross features of many such spectra can be reproduced [9]. In the case of one proton and one neutron in identical orbits the different states of the multiplet will alternate between  $T = 0$  and  $T = 1$  coupling depending on whether the total angular momentum is even or odd. Therefore the splitting of the states in the multiplet is directly sensitive to the magnitude of the  $T = 0$  pairing interaction.

In this work we consider the available experimental data for multiplets and calculate the corresponding states using the pnQRPA formalism. The strength of the  $T = 0$  pairing interaction is taken as a free parameters and is tuned in order to reproduce the experimental multiplet splittings.

This paper is organized as follows: in Sec. II the pnQRPA formalism is briefly reviewed and specific aspects of our formulation are discussed. In Sec III the computational cost and accuracy of the method is evaluated. In Sec. IV we discuss the experimental data. In sec. V the method is applied to the calculation of multiplet energies in a selection of odd-odd nuclei. Finally conclusions are given in section VI.

## II. THEORETICAL MODEL

In matrix form the QRPA equation [4, 10] can be expressed as

$$\hbar\omega \begin{pmatrix} X \\ -Y \end{pmatrix} = \begin{pmatrix} A & B \\ B^* & A^* \end{pmatrix} \begin{pmatrix} X \\ Y \end{pmatrix}, \quad (1)$$

---

\*Electronic address: gillis.carlsson@matfys.lth.se

where the  $A$  and  $B$  matrices have dimensions the size of two-body matrix elements. In order to avoid constructing and storing the large QRPA matrix it is useful to write the action of the matrix on the QRPA vectors in terms of transitional fields [2, 3]. This allows the action of the QRPA matrix on a vector to be constructed in a three step procedure [2, 3].

1. In the first step transitional densities are built as:

$$\tilde{\rho} = U \tilde{Z} V^T + V^* \tilde{Z}'^\dagger U^\dagger \quad (2)$$

$$\tilde{\kappa} = U \tilde{Z} U^T + V^* \tilde{Z}'^\dagger V^\dagger \quad (3)$$

$$\tilde{\kappa}'^\dagger = V \tilde{Z} V^T + U^* \tilde{Z}'^\dagger U^\dagger \quad (4)$$

where  $U$  and  $V$  denotes the matrices of the Bogoliubov transformation [10].  $\tilde{Z}$  and  $\tilde{Z}'^\dagger$  are anti-symmetric matrices whose upper triangular parts correspond to the elements in the  $X$  and  $Y$  column vectors.

2. In the second step the transitional fields are built. In the absence of a density-dependent pairing interaction they take the form:

$$\tilde{h}_{\mu\nu} = \sum_{\pi\lambda} \left. \frac{\partial h_{\mu\nu}}{\partial \rho_{\pi\lambda}} \right|_{\rho_{\text{gs}}} \tilde{\rho}_{\pi\lambda} = \sum_{\pi\lambda} \tilde{v}_{\mu\lambda\nu\pi} \tilde{\rho}_{\pi\lambda}, \quad (5)$$

$$\tilde{\Delta}_{\mu\nu} = \frac{1}{2} \sum_{kl} v_{\mu\nu kl}^{\text{pair}} \tilde{\kappa}_{kl}, \quad (6)$$

$$(\tilde{\Delta}'^\dagger)_{\mu\nu} = \frac{1}{2} \sum_{kl} v_{\mu\nu kl}^{\text{pair}*} (\tilde{\kappa}'^\dagger)_{kl}. \quad (7)$$

In these expressions, the matrix elements entering the  $\tilde{h}$  expression denotes the effective RPA interaction [10] while  $v_{\mu\nu kl}^{\text{pair}}$  denotes the pairing two-body matrix elements. In our case the Skyrme interaction is used as a particle-hole interaction and a separable interaction is used as a pairing interaction. With these special interactions, standard methods [2, 11] can be used to construct the fields which means that one can avoid constructing large matrices of two-body elements.

3. In the third step, these fields are multiplied with the Bogoliubov matrices to form the  $\tilde{W}$  matrices:

$$\tilde{W} = U^\dagger \tilde{h} V^* + U^\dagger \tilde{\Delta} U^* + V^\dagger \tilde{\Delta}'^\dagger V^* - V^\dagger \tilde{h}^T U^* \quad (8)$$

$$\tilde{W}'^\dagger = V^T \tilde{h} U + V^T \tilde{\Delta} V + U^T \tilde{\Delta}'^\dagger U - U^T \tilde{h}^T V. \quad (9)$$

It should be noted that the steps of building the transitional densities and fields are analogous to the way of building the HFB densities and fields and can thus be performed with slight modifications to an existing HFB code. Once these steps are completed the QRPA equations can be formulated as [2, 3]:

$$\hbar\omega \tilde{Z} = E \tilde{Z} + \tilde{Z} E + \tilde{W} \quad (10)$$

$$-\hbar\omega \tilde{Z}'^\dagger = E \tilde{Z}'^\dagger + \tilde{Z}'^\dagger E + \tilde{W}'^\dagger \quad (11)$$

where  $E$  denotes a diagonal matrix composed of the positive eigenvalues to the HFB equation [2, 3].

In our case when the HFB  $U$  and  $V$  matrices [10] do not mix neutrons and protons, these equations can be divided into two separate uncoupled pieces where one is the standard pp-nnQRPA equation and the other piece is the pnQRPA equation. To simplify the notation for the pnQRPA equation we first introduce the matrices:

$$\tilde{Z} = \begin{pmatrix} z_1 & z_2 \\ z_3 & z_4 \end{pmatrix}, \quad \tilde{Z}'^\dagger = \begin{pmatrix} \hat{z}_1 & \hat{z}_2 \\ \hat{z}_3 & \hat{z}_4 \end{pmatrix} \quad (12)$$

$$\tilde{W} = \begin{pmatrix} w_1 & w_2 \\ w_3 & w_4 \end{pmatrix}, \quad \tilde{W}'^\dagger = \begin{pmatrix} \hat{w}_1 & \hat{w}_2 \\ \hat{w}_3 & \hat{w}_4 \end{pmatrix}. \quad (13)$$

The grouping into four blocks is obtained from ordering the indexes so that proton states comes before neutron states. Then for example in the  $z_2$  and  $\hat{z}_2$  matrices, the first index refers to a proton state and the second one to a neutron state. A similar notation is used for the  $\tilde{\kappa}$ ,  $\tilde{\kappa}'^\dagger$  and the  $\tilde{\rho}$  matrices. In the same way the  $U$ ,  $V$  and  $E$  matrices also obtain block structures:

$$U = \begin{pmatrix} U_p & 0 \\ 0 & U_n \end{pmatrix}, \quad V = \begin{pmatrix} V_p & 0 \\ 0 & V_n \end{pmatrix}, \quad E = \begin{pmatrix} E_p & 0 \\ 0 & E_n \end{pmatrix}. \quad (14)$$

With this notation the pnQRPA part of the equation can be expressed:

$$\hbar\omega z_2 = E_p z_2 + z_2 E_n + w_2 \quad (15)$$

$$-\hbar\omega \hat{z}_2 = E_p \hat{z}_2 + \hat{z}_2 E_n + \hat{w}_2. \quad (16)$$

Since the Bogoliubov transformation preserves the proton and neutron quantum numbers we obtain:

$$w_2 = U_p^\dagger h_2 V_n^* + U_p^\dagger \Delta_2 U_n^* + V_p^\dagger \hat{\Delta}_2 V_n^* - V_p^\dagger h_3^T U_n^* \quad (17)$$

$$\hat{w}_2 = V_p^T h_2 U_n + V_p^T \Delta_2 V_n + U_p^T \hat{\Delta}_2 U_n - U_p^T h_3^T V_n \quad (18)$$

and

$$(h_2)_{pn} = \sum_{n'p'} \tilde{v}_{pn',np'}(\rho_2)_{p'n'} \quad (19)$$

$$(h_3)_{np} = \sum_{n'p'} \tilde{v}_{np',pn'}(\rho_3)_{n'p'} \quad (20)$$

$$(\Delta_2)_{pn} = \sum_{p'n'} v_{pn,p'n'}^{\text{pair}}(\kappa_2)_{p'n'} \quad (21)$$

$$(\hat{\Delta}_2)_{pn} = \sum_{p'n'} v_{pn,p'n'}^{\text{pair}*}(\hat{\kappa}_2)_{p'n'} \quad (22)$$

where the  $p$  and  $p'$  ( $n$  and  $n'$ ) indexes refer to proton (neutron) states. The relevant blocks of the transitional densities are obtained as

$$\rho_2 = U_p z_2 V_n^T + V_p^* \hat{z}_2 U_n^\dagger \quad (23)$$

$$\rho_3 = -U_n z_2^T V_p^T - V_n^* \hat{z}_2^T U_p^\dagger \quad (24)$$

$$\kappa_2 = U_p z_2 U_n^T + V_p^* \hat{z}_2 V_n^\dagger \quad (25)$$

$$\hat{\kappa}_2 = V_p z_2 V_n^T + U_p^* \hat{z}_2 U_n^\dagger. \quad (26)$$

The equations involve matrix elements of the Skyrme interaction in the  $T = 1$  and  $T_Z = \pm 1$  channels that are not active during standard HFB calculations which do not mix protons and neutrons. The evaluation of the extra matrix elements thus requires an extension of the usual method and this extension will be discussed in the next section.

### A. Evaluation of fields

With the Skyrme functional, and in the spin and isospin coupled notation the potential energy arising from the density-independent two-body part of the interaction can be expressed [11, 12]

$$\begin{aligned} \mathcal{E} &= \int \sum_{\alpha\beta t} C_{\alpha,J}^{t,\beta} \left[ [\rho_{\beta,J}^t, \rho_{\alpha,J}^t]_0^0 \right] d\mathbf{r} \\ &= \int \sum_{\alpha\beta t} C_{\alpha,J}^{t,\beta} \sum_{\substack{m_t m'_t \\ MM'}} C_{tm_t, tm'_t}^{00} C_{JM, JM'}^{00} \\ &\quad \times \rho_{\beta, JM}^{tm_t}(\mathbf{r}) \rho_{\alpha, JM'}^{tm'_t}(\mathbf{r}) d\mathbf{r}. \end{aligned} \quad (27)$$

In this expression vector (isovector) coupling is denoted by the square brackets with subscripts (superscripts) giving the value of the total spin (isospin). The coefficients  $C_{\alpha,J}^{t,\beta}$  denote the coupling constants of the model while e.g.  $C_{tm_t, tm'_t}^{00}$  denote Clebsch-Gordan coefficients [13]. The local densities entering this expression are defined as

$$\begin{aligned} \rho_{\alpha, JM}^{tm_t}(\mathbf{r}) &= \rho_{mI, nL\nu J', JM}^{tm_t}(\mathbf{r}) \\ &= \left[ \hat{D}_{mI}, \left[ \hat{K}_{nL}, \rho_{\nu}^{tm_t}(\mathbf{r}, \mathbf{r}') \right]_{J'} \right]_{J'} \Big|_{\mathbf{r}'=\mathbf{r}} \Big|_{JM}. \end{aligned} \quad (28)$$

In this expression  $\hat{D}_{mIM}$  ( $\hat{K}_{nLM}$ ) denote derivative operators (relative momentum operators) coupled to spherical tensors introduced in [11, 14]. To keep the notation simple we have introduced the label  $\alpha$  that stands for the set of quantum numbers  $\alpha = \{mI, nL\nu J'\}$ .

The local densities depend on the spin-isospin one-body density defined as

$$\begin{aligned} \rho_{\nu m_\nu}^{tm_t}(\mathbf{r}, \mathbf{r}') &= \sum_{\tau\tau'\sigma\sigma'} \rho(\mathbf{r}\tau\sigma, \mathbf{r}'\tau'\sigma') \\ &\quad \times \langle \sigma' | \hat{\sigma}_{\nu m_\nu} | \sigma \rangle \langle \tau' | \hat{\sigma}_{tm_t} | \tau \rangle \\ &= \sum_{\tau\tau'\sigma\sigma'} \sum_{b,b'} \phi_b(\mathbf{r}\sigma) \rho_{b\tau, b'\tau'} \phi_{b'}^*(\mathbf{r}'\sigma') \\ &\quad \times \langle \sigma' | \hat{\sigma}_{\nu m_\nu} | \sigma \rangle \langle \tau' | \hat{\sigma}_{tm_t} | \tau \rangle. \end{aligned} \quad (29)$$

In this expression the label  $b$  stands for the quantum numbers needed to specify the basis states. For example in the case of a harmonic oscillator basis  $b = \{Nljm\}$ . We assume the same basis states for neutrons and protons. The quantum number  $\tau$  ( $\sigma$ ) is the isospin (spin) projection. For the Pauli matrices we use the tensor form of the operators introduced in Eq. 14 and 15 of [11]. Introducing the short-hand notation  $\langle \sigma' | \hat{\sigma}_{\nu m_\nu} | \sigma \rangle = \sigma_{\nu m_\nu}^{\sigma'\sigma}$  the explicit relations for the different components of the one-body density can be written as:

$$\begin{aligned} \rho_{\nu m_\nu}^{00}(\mathbf{r}, \mathbf{r}') &= \sum_{\sigma\sigma'bb'} \phi_b(\mathbf{r}\sigma) \phi_{b'}^*(\mathbf{r}'\sigma') \sigma_{\nu m_\nu}^{\sigma'\sigma} \\ &\quad \times \left( \rho_{b-\frac{1}{2}, b'-\frac{1}{2}} + \rho_{b\frac{1}{2}, b'\frac{1}{2}} \right) \end{aligned} \quad (30)$$

$$\begin{aligned} \rho_{\nu m_\nu}^{10}(\mathbf{r}, \mathbf{r}') &= \sum_{\sigma\sigma'bb'} \phi_b(\mathbf{r}\sigma) \phi_{b'}^*(\mathbf{r}'\sigma') \sigma_{\nu m_\nu}^{\sigma'\sigma} \\ &\quad \times (-i) \left( \rho_{b\frac{1}{2}, b'\frac{1}{2}} - \rho_{b-\frac{1}{2}, b'-\frac{1}{2}} \right) \end{aligned} \quad (31)$$

$$\begin{aligned} \rho_{\nu m_\nu}^{1-1}(\mathbf{r}, \mathbf{r}') &= \sum_{\sigma\sigma'bb'} \phi_b(\mathbf{r}\sigma) \phi_{b'}^*(\mathbf{r}'\sigma') \sigma_{\nu m_\nu}^{\sigma'\sigma} \\ &\quad \times (-i) \left( \sqrt{2} \rho_{b\frac{1}{2}, b'-\frac{1}{2}} \right) \end{aligned} \quad (32)$$

$$\begin{aligned} \rho_{\nu m_\nu}^{11}(\mathbf{r}, \mathbf{r}') &= \sum_{\sigma\sigma'bb'} \phi_b(\mathbf{r}\sigma) \phi_{b'}^*(\mathbf{r}'\sigma') \sigma_{\nu m_\nu}^{\sigma'\sigma} \\ &\quad \times (-i) \left( -\sqrt{2} \rho_{b-\frac{1}{2}, b'\frac{1}{2}} \right) \end{aligned} \quad (33)$$

We take protons to have isospin  $\tau = -1/2$  so Eq. 30 says e.g. that the isoscalar part of the one-body density involves the sum of the proton and neutron density matrices. Expanding the isospin coupling in Eq. 27 gives

$$\begin{aligned} \mathcal{E} &= \int d\mathbf{r} \sum_{\alpha\beta, J} C_{\alpha,J}^{0,\beta} [\rho_{\beta,J}^{00}, \rho_{\alpha,J}^{00}]_0 \\ &\quad - \frac{C_{\alpha,J}^{1,\beta}}{\sqrt{3}} [\rho_{\beta,J}^{10}, \rho_{\alpha,J}^{10}]_0 \\ &\quad + \frac{C_{\alpha,J}^{1,\beta}}{\sqrt{3}} \left( [\rho_{\beta,J}^{11}, \rho_{\alpha,J}^{1-1}]_0 + [\rho_{\beta,J}^{1-1}, \rho_{\alpha,J}^{11}]_0 \right). \end{aligned} \quad (34)$$

To make the expression more symmetric we introduce new local densities

$$\rho_{\alpha, JM}^+(\mathbf{r}) = \rho_{\alpha, JM}^{11}(\mathbf{r}) + \rho_{\alpha, JM}^{1-1}(\mathbf{r}) \quad (35)$$

$$\rho_{\alpha, JM}^-(\mathbf{r}) = \rho_{\alpha, JM}^{11}(\mathbf{r}) - \rho_{\alpha, JM}^{1-1}(\mathbf{r}) \quad (36)$$

which gives

$$\begin{aligned}\mathcal{E} = & \int d\mathbf{r} \sum_{\alpha\beta} C_{\alpha,J}^{0,\beta} [\rho_{\beta,J}^{00}, \rho_{\alpha,J}^{00}]_0 \\ & - \frac{C_{\alpha,J}^{1,\beta}}{\sqrt{3}} [\rho_{\beta,J}^{10}, \rho_{\alpha,J}^{10}]_0 \\ & + \frac{C_{\alpha,J}^{1,\beta}}{\sqrt{3}} \frac{1}{2} \left( [\rho_{\beta,J}^+, \rho_{\alpha,J}^+]_0 - [\rho_{\beta,J}^-, \rho_{\alpha,J}^-]_0 \right). \quad (37)\end{aligned}$$

The new local densities can be considered to be built from the density matrices

$$\rho_{\nu m_\nu}^+(\mathbf{r}, \mathbf{r}') = \sum_{\sigma\sigma'b,b'} \phi_b(\mathbf{r}\sigma) \phi_{b'}^*(\mathbf{r}'\sigma') \sigma_{\nu m_\nu}^{\sigma'\sigma} \rho_{b,b'}^+ \quad (38)$$

$$\rho_{\nu m_\nu}^-(\mathbf{r}, \mathbf{r}') = \sum_{\sigma\sigma'b,b'} \phi_b(\mathbf{r}\sigma) \phi_{b'}^*(\mathbf{r}'\sigma') \sigma_{\nu m_\nu}^{\sigma'\sigma} \rho_{b,b'}^-, \quad (39)$$

where

$$\rho_{b,b'}^+ = i\sqrt{2} \left( \rho_{b-\frac{1}{2},b'+\frac{1}{2}} - \rho_{b\frac{1}{2},b'-\frac{1}{2}} \right) \quad (40)$$

$$\rho_{b,b'}^- = i\sqrt{2} \left( \rho_{b-\frac{1}{2},b'+\frac{1}{2}} + \rho_{b\frac{1}{2},b'-\frac{1}{2}} \right). \quad (41)$$

The new fields needed for pnQRPA have  $\tau \neq \tau'$  and can be written

$$\begin{aligned}h_{b\tau,b'\tau'} &= \frac{\partial \mathcal{E}}{\partial \rho_{b'\tau',b\tau}} \\ &= \frac{\partial \mathcal{E}}{\partial \rho_{b',b}^+} \frac{\partial \rho_{b',b}^+}{\partial \rho_{b'\tau',b\tau}} + \frac{\partial \mathcal{E}}{\partial \rho_{b',b}^-} \frac{\partial \rho_{b',b}^-}{\partial \rho_{b'\tau',b\tau}} \\ &= i\sqrt{2} \left( \frac{\partial \mathcal{E}}{\partial \rho_{b',b}^+} 2\tau + \frac{\partial \mathcal{E}}{\partial \rho_{b',b}^-} \right). \quad (42)\end{aligned}$$

Thus the main task is calculating the fields

$$\begin{aligned}\Gamma_{bb'}^+ &= \frac{\partial \mathcal{E}}{\partial \rho_{b',b}^+} \\ &= \frac{1}{2} \frac{\partial}{\partial \rho_{b',b}^+} \int d\mathbf{r} \sum_{\alpha\beta,J} \frac{C_{\alpha,J}^{1,\beta}}{\sqrt{3}} [\rho_{\beta,J}^+, \rho_{\alpha,J}^+]_0 \quad (43)\end{aligned}$$

and

$$\begin{aligned}\Gamma_{bb'}^- &= \frac{\partial \mathcal{E}}{\partial \rho_{b',b}^-} \\ &= \frac{-1}{2} \frac{\partial}{\partial \rho_{b',b}^-} \int d\mathbf{r} \sum_{\alpha\beta,J} \frac{C_{\alpha,J}^{1,\beta}}{\sqrt{3}} [\rho_{\beta,J}^-, \rho_{\alpha,J}^-]_0. \quad (44)\end{aligned}$$

Except for the constants  $\frac{1}{2}$  and  $-\frac{1}{2}$  these fields have the same form as the fields resulting from the isovector term. Thus the same computer routines can be reused for the calculation of these new terms.

## B. Density-dependent interaction

Introducing a standard scalar-isoscalar density dependence gives the new term

$$\mathcal{E}^{dd} = \sum_{\alpha\beta} \frac{C_{\alpha,J}^{1,\beta}}{\sqrt{3}} \rho_0^\alpha \frac{1}{2} \left( [\rho_{\beta,J}^+, \rho_{\alpha,J}^+]_0 - [\rho_{\beta,J}^-, \rho_{\alpha,J}^-]_0 \right). \quad (45)$$

One realizes that variations of the type

$$\left. \frac{\partial^2 \mathcal{E}^{dd}}{\partial \rho_{bb'}^x \partial \rho_{cc'}^x} \right|_{\rho=\rho_{\text{gs}}} \quad (46)$$

where  $x = +$  or  $-$  will give rise to non-zero contributions and other variations will not give anything. This is because the  $\rho_{bb'}^+$  and  $\rho_{bb'}^-$  density matrices are zero in the ground state when protons and neutrons are uncorrelated. Therefor one only obtains contributions to the fields

$$\tilde{\Gamma}_{ij} = \sum_{kl} \tilde{v}_{iljk} \tilde{\rho}_{kl}, \quad (47)$$

where one of the indexes  $i, j$  refers to a proton and the other one to a neutron. This means that we must consider the matrix elements  $\tilde{v}_{pn'np'}$  and  $\tilde{v}_{np'pn'}$  since the other combinations where the first two indexes refer to the same particle species are forbidden by charge conservation. The first of these matrix elements can be expressed [10]

$$\begin{aligned}\tilde{v}_{pn'np'} &= \left. \frac{\partial E_{HF}}{\partial \rho_{np} \partial \rho_{p'n'}} \right|_{\rho_{\text{gs}}} \\ &= \bar{v}_{n'pp'n}[\rho] + \sum_{jl} \rho_{lj} \left( \frac{\partial \bar{v}_{n'jp'l}[\rho]}{\partial \rho_{np}} + \frac{\partial \bar{v}_{pjnl}[\rho]}{\partial \rho_{p'n'}} \right) \Bigg|_{\rho_{\text{gs}}} \\ &+ \frac{1}{2} \sum_{ijkl} \rho_{ki} \frac{\partial \bar{v}_{ijkl}[\rho]}{\partial \rho_{p'n'} \partial \rho_{np}} \rho_{lj} \Bigg|_{\rho_{\text{gs}}} \\ &= \bar{v}_{n'pp'n}[\rho_{\text{gs}}]. \quad (48)\end{aligned}$$

The last line follows since the density-dependence is explicitly with respect to the isoscalar density so the variations of the matrix elements with respect to the mixed proton-neutron densities become zero. For the  $\tilde{v}_{np'pn'}$  combination it works in the same way. Thus with the standard isoscalar  $\rho_0^\alpha$  density-dependence there are no additional rearrangement terms appearing in the pn-QRPA.

## C. Pairing interaction

For the pairing interaction we adopt a form:

$$V(\mathbf{r}_1, \mathbf{r}_2, \mathbf{r}'_1, \mathbf{r}'_2) = \delta(\mathbf{R} - \mathbf{R}') P(r) P(r') \times [G_1 \hat{\Pi}_{s=0} + G_0 \hat{\Pi}_{S=1, T=0}] \quad (49)$$

where

$$P(r) = \frac{1}{(4\pi a^2)^{3/2}} e^{-r^2/(4a^2)} \quad (50)$$

$$\hat{\Pi}_{s=0} = \frac{1}{2} (1 - P^\sigma) \quad (51)$$

$$\hat{\Pi}_{S=1, T=0} = \frac{1}{4} (1 + P^\sigma) (1 - P^\tau). \quad (52)$$

Since this interaction has a finite range it leads to convergent results and no energy cut-off is needed for the pairing space. The separable structure of the interaction allows an efficient evaluation of the two-body matrix elements [2]. The isovector part of this interaction was first considered in [15] to parameterize the bare low-momentum potential in the  $^1S_0$  channel. Here the parameterization is straightforwardly extended to the  $T = 0$  channel assuming the same radial dependence.

### III. ACCURACY AND CONVERGENCE

In order to find the eigenvalues of the large pnQRPA matrix we use the Implicitly Restarted Arnoldi method (IRA) [16, 17]. With this approach the pnQRPA matrix never has to be built, it is sufficient to be able to calculate the results of the matrix acting on an arbitrary vector which can be done as outlined in the previous section. The method is implemented in an updated version of the HOSPHE (v1.02) [11] code.

An example of the calculations is shown in

Fig. 1. In this figure we have selected the lowest multiplet states in the nucleus  $^{51}\text{Sb}_{83}$  that has a proton-neutron pair outside closed shells. The proton neutron pair is assumed to be in a  $\pi g_{7/2} \otimes \nu f_{7/2}$  configuration and the corresponding excitations are extracted from the code requesting the states where this configuration has the largest amplitude. The longest time is spent on calculating the highest angular momentum states. For the  $I = 7^-$  calculation with  $N_{max} = 16$  it takes about 6.5 min on a standard desktop computer (Intel Core i7-2600K, 3.4GHz). The time depends on the requested accuracy as well as the number of requested converged excitations. In this case the 15 lowest positive energy pnQRPA excitations was requested and set to be converged with a tolerance parameter [18] of  $10^{-6}$ . As seen from Fig. 1, the relative energies of the multiplet states converge rapidly with increasing number of oscillator shells.  $N_{max} = 16$  appears to give a sufficient accuracy and will therefore be used in the following.

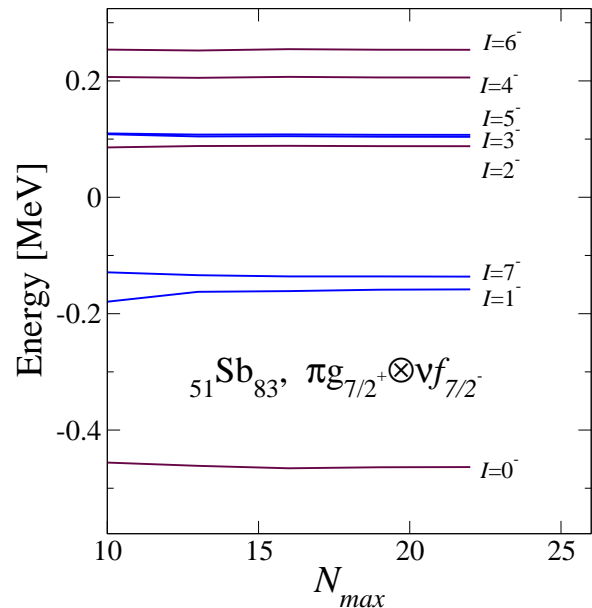


Figure 1: (Color online) Convergence of the relative energies of the low-lying multiplet in  $^{51}\text{Sb}_{83}$  as a function of the maximum oscillator shell  $N_{max}$  included in the basis. The energies are drawn relative to the average energy of the multiplet. The SKX Skyrme interaction [19] was used with pairing parameters  $(G_1, G_0) = (545, 763) \text{ MeVfm}^3$  ( $G_0/G_1=1.4$ ).

### IV. SELECTION OF EXPERIMENTAL DATA

Starting from double-magic spherical nuclei we consider neighboring nuclei with an excited proton-neutron pair of particles or holes. The proton-neutron pair can couple to different total angular momentum values forming a multiplet of states. In order to identify the states we start by considering the experimental ground states of the odd nuclei surrounding the double magic one. From the ground state spins of the odd nuclei,  $j_p$  and  $j_n$  we can identify the corresponding configurations by comparing with a Nilsson diagram. Then the largest components in the lowest states of the odd-odd nuclei are assumed to result from the coupling of these states. In the case of  $N = Z$  nuclei the isospin of the states is sometimes experimentally determined. In these cases we apply the additional condition that for protons and neutrons in identical orbits, even (odd) $J$  must be combined with  $T = 1$  (0) in order to make the wave function anti symmetric [20]. Thus for the  $N = Z$  nuclei we make use of this relation and select the lowest experimental states that have isospin values consistent with those of our assumed configurations.

Nucleus	Configuration	$I^\pi$	$E_{exp}$	Remark
$^{18}_9\text{F}_9$	$\pi d_{5/2+} \otimes \nu d_{5/2+}$	$0^+$	1.04155	
		$1^+$	0	(a)
		$2^+$	3.06184	
		$3^+$	0.93720	(a)
		$4^+$	4.65200	
$^{42}_{21}\text{Sc}_{21}$	$\pi f_{7/2-} \otimes \nu f_{7/2-}$	$0^+$	0	
		$1^+$	0.611051	
		$2^+$	1.58631	
		$(3^+)$	1.49043	
		$4^+$	1.12136	
$^{50}_{21}\text{Sc}_{29}$	$\pi f_{7/2-} \otimes \nu p_{3/2-}$	$0^+$	0	
		$1^+$	0.611051	
		$2^+$	1.58631	
		$(3^+)$	1.49043	
		$4^+$	1.12136	
$^{58}_{29}\text{Cu}_{29}$	$\pi p_{3/2-} \otimes \nu p_{3/2-}$	$0^+$	0.202990	
		$1^+$	0	
		$2^+$	1.6525	
		$(3^+)$	0.443640	
		$4^+$	1.12136	
$^{134}_{51}\text{Sb}_{83}$	$\pi g_{7/2+} \otimes \nu f_{7/2-}$	$0^+$	0	
		$1^-$	0.0130	
		$2^-$	0.3311	
		$3^-$	0.3840	
		$4^-$	0.5550	
		$5^-$	0.441	
		$6^-$	0.617	
		$7^-$	0.279	
		$(1^-)$	0.8850	
		$(2^-)$	0.9350	
	$\pi d_{5/2+} \otimes \nu f_{7/2-}$	$1^-$	0.8850	
		$2^-$	0.9350	
		$3^-$		
		$4^-$		
		$5^-$		
		$6^-$		

$^{210}_{83}\text{Bi}_{127}$  see caption

Table I: Experimental data [21] for nuclei with a proton-neutron pair outside closed shells. The experimental states considered are listed along with their assumed largest configurations. For  $^{210}_{83}\text{Bi}_{127}$  we have adopted the first seven multiplets shown in Table III of Ref. [22] along with the suggested 58 corresponding experimental energies. All energies are in MeV.

In this way tables I and II are constructed. Table I contains data for particle states and table II contains data for hole states. In addition to these tables, Ref. [22] contains a table of 13 identified experimental multiplets in  $^{210}_{83}\text{Bi}_{127}$ . As part of the data set we adopt the first 7 multiplets shown in Table III of Ref. [22].

Nucleus	Configuration	$I^\pi$	$E_{exp}$	Remark
$^{14}_7\text{N}_7$	$\pi p_{1/2-} \otimes \nu p_{1/2-}$	$0^+$	2.312798	
		$1^+$	0	
$^{38}_{19}\text{K}_{19}$	$\pi d_{3/2+} \otimes \nu d_{3/2+}$	$0^+$	0.1304	
		$1^+$	1.698	
		$2^+$	2.40107	
		$3^+$	0	
$^{46}_{19}\text{K}_{27}$	$\pi d_{3/2+} \otimes \nu f_{7/2-}$	$(2^-)$	0	
		$3^-$	0.5874	(a)
		$(4^-)$	0.6909	(a)
		$5^-$	0.8855	
$^{54}_{27}\text{Co}_{27}$	$\pi f_{7/2-} \otimes \nu f_{7/2-}$	$0^+$	0	
		$1^+$	0.93690	
		$2^+$	1.44566	
		$3^+$	1.82149	
		$4^+$	2.65197	(b)
		$(5^+)$	1.8870	
$^{130}_{49}\text{In}_{81}$	$\pi g_{9/2+} \otimes \nu h_{11/2-}$	$(6^+)$	2.979	(b)
		$7^+$	0.1970	
		$(1^-)$	0.0000	
		$2^-$		
		$3^-$		
		$4^-$		
		$5^-$		
		$6^-$		
		$7^-$		
		$8^-$		
		$9^-$		
		$(10^-)$	0.0500	

Table II: Same as Table I but for nuclei with a proton-neutron hole-pair outside closed shells. Levels marked with (a) may belong to the multiplet  $\pi s_{1/2+} \otimes \nu f_{7/2-}$ .

In some cases it is possible to compare our assumed assignments for the largest wave function configurations with previous shell-model calculations. In the case of  $^{18}\text{F}$  shell-model calculations [23] confirm our assumptions about the largest amplitude configurations except for the  $1^+$  and  $3^+$  states where the largest components are suggested to be  $\pi d_{5/2}\nu d_{3/2}$  and  $\pi d_{5/2}\nu s_{1/2}$  configurations. These two states marked with (a) in Tab. I are thus excluded from the data set. For  $^{42}\text{Sc}$  our assumption about the largest amplitude configurations is confirmed by shell-model calculations [24]. In  $^{50}\text{Sc}$  there are two possible spin assignments for the second state of the multiplet. Previous comparisons with shell-model calculations [25] suggest the  $2^+$  interpretation we adopt here as well. In the case of  $^{134}\text{Sb}$ , the spin values are shown in parenthesis indicating that they are not directly measured but comparisons with shell model calculations [26] support the experimental spin assignments given for the two observed multiplets in this nucleus.

In the case of hole states shown in Tab. II and for  $^{38}\text{K}$  we have chosen the second observed  $1^+$  state that exper-

iments suggests to be the one with largest  $d_{3/2}$  components [27]. For  $^{46}\text{K}$  we have excluded the  $3^-$  and the  $4^-$  states marked with (a) in Tab. II from the data set. That is because these states may also arise from a possible  $[\pi s_{1/2+}, \nu f_{7/2-}]_{3-,4-}$  coupling or may be a mixture of both of these multiplets. Although the pnQRPA takes this mixing into account we prefer to have as clean data as possible. In the case of  $^{54}\text{Co}$  we adopt the  $4^+$  and  $6^+$  states marked with (b) in Tab. II although there are lower states with tentative spin assignments that could belong to the multiplet. The decay patterns and comparisons with shell model calculations suggest the present interpretation [28]. With these selections we end up with a data set consisting of a total of 104 states.

## V. DETERMINATION OF THE ISOSCALAR PAIRING STRENGTH

In this article the values of the isovector pairing strengths and range parameter ( $a = 0.660$  fm) are considered to be fixed from values used in our previous study [3]. In Ref. [3] different strength was used for neutrons and protons but in this work we assume an isospin symmetric  $T = 1$  interaction with a strength given by the average of the proton and neutron values taken from [3]. In general the Coulomb interaction will introduce isospin breaking leading to different pairing strengths for protons and neutrons. In a complete approach one should thus also consider the Coulomb contribution to the pairing interaction. However, inclusion of Coulomb is problematic since approximate treatments may give rise to divergences, see e.g. [7], and exact treatments becomes time-consuming. Since the objective of this work is to determine a first value of the  $T = 0$  pairing strength that can be used in pnQRPA calculations for  $\beta$ -decay, we have opted to start by investigating the simpler isospin invariant form.

When comparing experimental and theoretical states one should note that in the pnQRPA formalism the resulting excitations have preserved total angular momentum and parity but are in general composed of a mixture of 'pure' multiplet configurations such as those shown in Tabs. I and II. Thus in order to select the states that should be compared with data we extract the theoretical states that has the postulated experimental configurations as the largest amplitudes. In case there are two such theoretical states the one lowest in energy is selected.

### A. Full fits

In the case of a multiplet where all experimental states are not measured or some states are excluded on the basis of being uncertain we define the average energy of the multiplet as the average of the remaining experimental states. The average of the same theoretical states are then used to define the average theoretical energy of the

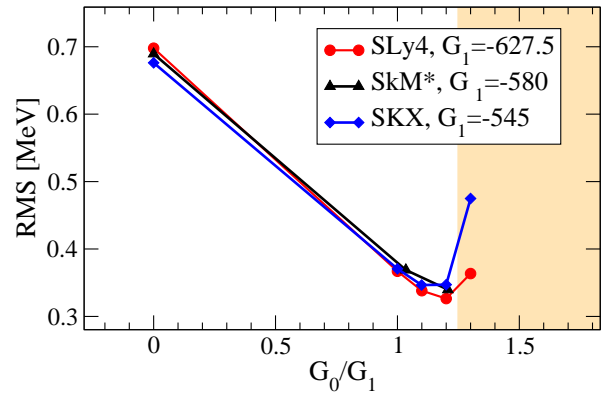


Figure 2: (Color online) RMS as a function of the  $G_0/G_1$  ratio. All 104 experimental states was used for the comparison.

multiplet. Since in general Skyrme interactions will produce errors of  $\sim 1.4$  MeV for single-particle energies [29] we do not compare the average energies with experiment. Instead the experimental and theoretical relative energies within the multiplet are compared and the RMS is taken as the difference between experimental and theoretical relative energies.

Fig. 2 shows the RMS as a function of the isoscalar pairing strength. The data set involved all 104 states and as seen in the figure the description of data becomes better as the strength is increased.

The curves in Fig. 2 are drawn until imaginary eigenvalues starts to appear in the pnQRPA calculations. For each interaction, starting from the last point on the curves and increasing the  $G_0/G_1$  ratio by 10 % leads to the appearance of such points. For all nuclei it seems that as the  $T = 0$  strength reaches a value  $G_0 \gtrsim 1.2G_1$  the pnQRPA starts to become unstable for  $N = Z$  nuclei. This may indicate that the ground state is not a stationary point with respect to proton-neutron correlations and may thus go through a transition into an isoscalar proton-neutron pairing condensate (see e.g. the discussion in Ref. [30]).

Both the SKX [19] and the SLy4 [31] interactions show minima at  $G_0/G_1 = 1.2$  and in both cases the increase in RMS when going to  $G_0/G_1 = 1.3$  can be traced to two  $N = Z$  nuclei ( $^{42}\text{Sc}$  and  $^{38}\text{K}$ ) whose errors increase substantially while the RMS for most of the remaining nuclei actually decreases. Further increasing the  $T = 0$  pairing strength to  $G_0/G_1 = 1.4$  leads to imaginary eigenvalues appearing in the  $J = 1^+$  channel for the same nuclei. At  $G_0/G_1 = 1.3$  and for the SKX interaction the lowest energy excitation in this channel is at 0.18 MeV while it is at 1.9 MeV with SLy4 indicating that the SLy4 minimum is more reliable while the last SKX point is likely too close to instability to be reliable.

The results for the SkM\* interaction [32] follows the other ones but reaches the unstable point before any tendency for a minimum is displayed.

In general the multiplet splitting is larger in the light nuclei and they therefor get more important when tuning

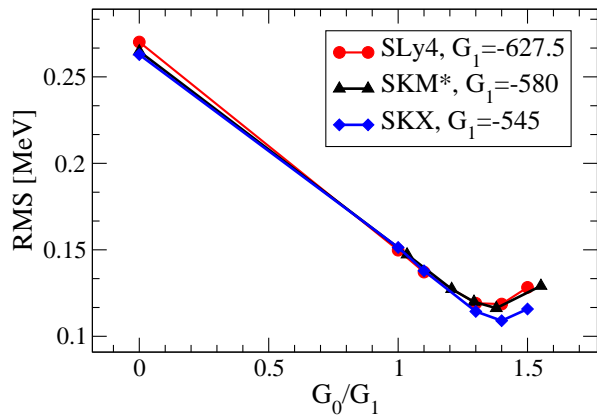


Figure 3: (Color online) RMS as a function of the  $G_0/G_1$  ratio. The comparison is performed using the 76 states remaining when  $N = Z$  nuclei are removed from the data set.

the strength. In order to remove this dependence one can divide the energies by  $41A^{-1/3}$  to obtain oscillator units [33] which removes the average energy dependence arising from the different stiffness of the nuclear potential for light and heavy nuclei. If the RMS is instead calculated in oscillator units the minimum obtained for SLy4 still occurs for the same interaction strength.

### B. Fits with a reduced data set

In order to be able to test a larger range of interaction strengths the  $Z = N$  nuclei are excluded from the fits leaving a total of 76 states. The result of this calculation is shown in

Fig. 3. As seen in this figure, when the  $N = Z$  nuclei are removed all the interactions produce minima when  $G_0 \simeq 1.4G_1$ . It is interesting to note that the obtained values are in good agreement with the ratio of isovector to isoscalar pairing of 1.3 that was found in Ref. [30] in order to describe the Wigner energy as a binding energy gain caused by  $T = 0$  pairing in the BCSLN model.

### C. Results for multiplets

The results from the optimal fit obtained with the SKX interaction and  $G_0 = 1.4G_1$  are shown for the largest multiplets in

figures 4 and 5. If it was not for the the isoscalar and isovector pairing interactions the resulting theoretical curves would become constant with the value 0. Thus no splitting of the multiplets would be predicted. Including a  $T = 1$  pairing interaction results in the dashed curves in Figs. 4 and 5. These curves obtain some staggering that makes them agree better with experiment.

With the  $T = 0$  pairing interaction added, shown with full drawn curves in figures 4 and 5, the description shows

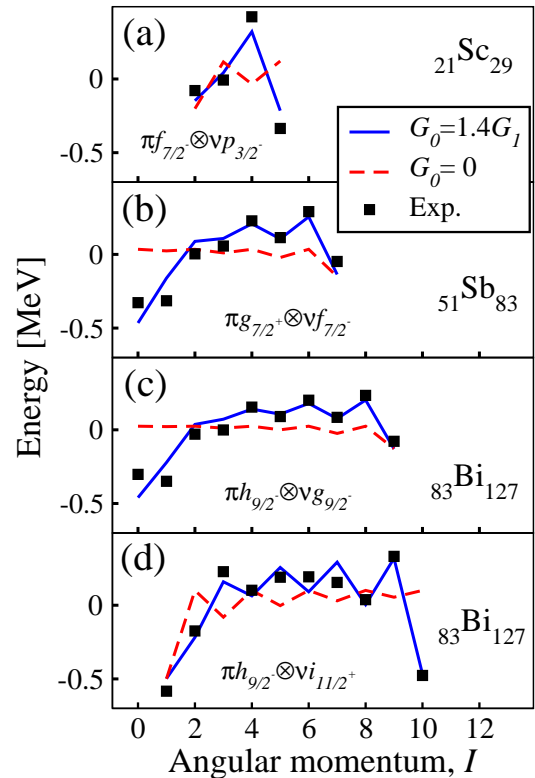


Figure 4: (Color online) Relative energies of the largest  $N \neq Z$  multiplets calculated using the SKX interaction and compared with experiment.

a considerable improvement and the theoretical multiplet splittings are in good agreement with experiment.

For the  $^{21}\text{Sc}_{29}$  nucleus the lowest multiplet is expected to result from a  $\pi (f_{7/2})^1 \nu (p_{3/2})^1$  configuration which can couple to  $I = 2^+ - 5^+$  [25]. As seen from panel (a) in Fig. 4, the ordering of the states is correctly described and the relative energies compare well with experiment. The lowest multiplet in  $^{51}\text{Sb}_{83}$  was previously described in the shell-model approach using experimental single-particle levels and an effective interaction derived from the CD-Bonn  $NN$  potential [26]. The biggest discrepancy was obtained for the  $7^-$  state which was predicted about 130 keV above the experimental state. In our case, the  $7^-$  state shown in panel (b) of Fig. 5 is instead predicted about 130 keV below the experimental state. However it should also be noted that in Ref. [26] the energies are normalized to the lowest state in the multiplet while in this work we normalize to the average multiplet energy. The most striking difference between the calculations is that while we overpredict the relative energies of the  $0^-$  and  $1^-$  states, the shell model calculation gave almost the correct energy splitting between these states. The same



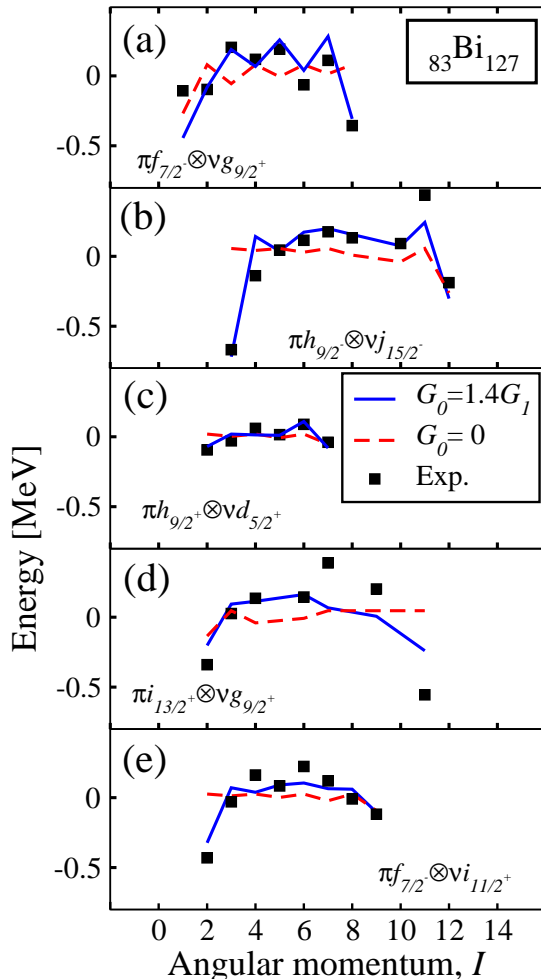


Figure 5: (Color online) Same as Fig. 4 for additional multiplets.

discrepancy is also seen in  $^{83}\text{Bi}_{127}$  (see panel (c) of Fig. 4) where the  $0^-$  state comes out lowest in our calculation while the experimental ground state is  $1^-$ . Both shell model calculations based on realistic interactions [34] and phenomenological forces that include non-central tensor and spin-orbit terms can give the correct ordering [22]. For example in Ref. [22] a phenomenological force with 8 free parameters was fitted to multiplet data in  $^{83}\text{Bi}_{127}$  which lead to a good reproduction of the spectra. This suggests that a more complicated interaction could give a better description of the data but rather than introducing additional parameters it seems more interesting to attempt to constrain the  $T = 0$  effective force starting from bare interactions as done for the  $T = 1$  part in Ref.

[15]. However this work is left as a future exercise.

In Fig. 5 the description of the higher lying multiplets in  $^{83}\text{Bi}_{127}$  is shown. A few more multiplets have been identified [22] but here we have restricted us to those with the lowest excitation energies since the mixing with configurations that are outside the scope of the pnQRPA description are expected to increase with increasing excitation energy.

## VI. SUMMARY AND CONCLUSIONS

An iterative method for the solution of the pnQRPA equations that avoids the construction of the large pnQRPA matrix was introduced and employed for the calculation of low-lying states. The method uses the Implicitly Restarted Arnoldi approach for the solution of the non-hermitian eigenvalue problem. In this approach, only the action of the matrix on a Ritz vector is needed and this can be expressed in terms of effective fields generated by transitional densities. The numerical tests shows that the method is both fast and reliable. When generalizing the method to the pnQRPA case additional fields in the particle-hole channel which are not active in standard HFB calculations must be taken into account. The expressions for the new fields follow straightforwardly from the requirement that the nuclear interaction is invariant with respect to rotations in isospin space and we demonstrated how they may be calculated analogously to the standard isovector fields.

The excitations in the pnQRPA are proton and neutron quasiparticle pairs and the results become sensitive to whether these pairs like to pair up with their spins in parallel or anti-parallel. This feature is determined by the relative strengths of the  $T = 1$  and  $T = 0$  components of the pairing interaction. It should be noted that in recent fits of Skyrme interactions [35, 36] the  $T = 0$  pairing channel is not probed at all since proton-neutron pairing is generally neglected in the models. However for descriptions of  $\beta$ -decay [5, 6] and neutrinos that scatter on nuclei [37] the  $T = 0$  pairing channel has a large influence on the results.

In this work we considered a simple isospin invariant parameterization of the  $T = 1$  and  $T = 0$  pairing interactions and determined the  $T = 0$  pairing strength from multiplet data. The comparison with experimental data suggests that the effective pairing interaction in the  $T = 0$  channel should be roughly 40 % stronger than the  $T = 1$  pairing interaction. It is interesting that these values are in agreement with previous estimates of a 30 % stronger  $T = 0$  channel obtained from assuming the Wigner energy arises from proton-neutron pairing [30]. The collapse of the pnQRPA obtained for some of the  $N = Z$  nuclei further corroborates this view and may be indicative of a phase transition to a  $T = 0$  pairing condensate.

It should also be noticed that in a recent study [38] a reasonable agreement with experiment was obtained for

Wigner energies using an effective Hamiltonian without any isoscalar pairing. In fact the authors find that, with their model, ratios of isoscalar to isovector pairing larger than 0.8 does not lead to the correct mass differences.

It is not straightforward to compare the different studies since different many-body approaches and different interactions are generally employed. It would therefore be interesting to see if it is possible to find a common effective  $T = 0$  interaction compatible with all the different types of experimental data such as multiplet energies,  $\beta$ -decay probabilities, ground state energies etc.

Although the many-body approach of this work is more advanced, the structure of the pairing interactions assumed here is certainly simpler than those of some previous studies [22, 39]. However since the main features of the data can be described with the simple form used in this work, it may be taken as a first approximation to be used in future pnQRPA studies. In the long run the goal would be to determine better effective interactions

and preferably such interactions that have the same form in both in the particle-hole and the pairing channels. For such studies low-lying states in odd-odd nuclei can provide important constraints on the effective interactions.

## acknowledgments

B.G. Carlsson acknowledges D. Rudolph for discussions concerning the experimental data and the Royal Physiographic Society in Lund for providing funding for the computers on which the calculations were performed. We also thank R. Bengtsson for valuable comments on the manuscript. This work was supported in part by the Academy of Finland and University of Jyväskylä within the FIDIPRO programme. B.G.C thank the Swedish Research Council (VR) for financial support.

- 
- [1] J. Toivanen, B. G. Carlsson, J. Dobaczewski, K. Mizuyama, R. R. Rodríguez-Guzmán, P. Toivanen, and P. Veselý, Phys. Rev. C **81**, 034312 (2010).
  - [2] P. Veselý, J. Toivanen, B. G. Carlsson, J. Dobaczewski, N. Michel, and A. Pastore, Phys. Rev. C **86**, 024303 (2012).
  - [3] B. G. Carlsson, J. Toivanen, and A. Pastore, Phys. Rev. C **86**, 014307 (2012).
  - [4] J. Suhonen, *From Nucleons to Nucleus*, Springer-Verlag, Berlin Heidelberg, 2007.
  - [5] M. T. Mustonen and J. Engel, Phys. Rev. C **87**, 064302 (2013).
  - [6] J. Engel, M. Bender, J. Dobaczewski, W. Nazarewicz, and R. Surman, Phys. Rev. C **60**, 014302 (1999).
  - [7] B. G. Carlsson, J. Toivanen, and U. von Barth, Phys. Rev. C **87**, 054303 (2013).
  - [8] L. W. Nordheim, Phys. Rev. **78**, 294 (1950).
  - [9] J. Schiffer, Annals of Physics **66**, 798 (1971).
  - [10] P. Ring and P. Schuck, *The Nuclear Many-Body Problem* (1st ed. Springer-Verlag, New York, 1980).
  - [11] B. G. Carlsson, J. Dobaczewski, J. Toivanen, and P. Veselý, Comp. Phys. Commun. **181**, 1641 (2010).
  - [12] B. G. Carlsson and J. Dobaczewski, Phys. Rev. Lett. **105**, 122501 (2010).
  - [13] A.N. Varshalovich and A.N. Moskalev and V.K. Kheranskii, *Quantum Theory of Angular Momentum* (World Scientific, Singapore, 1988).
  - [14] B. G. Carlsson, J. Dobaczewski, and M. Kortelainen, Phys. Rev. C **78**, 044326 (2008).
  - [15] T. Duguet, Phys. Rev. C **69**, 054317 (2004).
  - [16] W. E. Arnoldi, Quarterly of Applied Mathematics **9**, 17 (1951).
  - [17] Y. Saad, Linear algebra and its applications **34**, 269 (1980).
  - [18] ARPACK: <http://www.caam.rice.edu/software/ARPACK/>.
  - [19] B. A. Brown, Phys. Rev. C **58**, 220 (1998).
  - [20] I. Talmi, *Simple Models of Complex Nuclei* (Harwood Academic Publishers, Chur, Switzerland, 1993).
  - [21] The ENSDF database: <http://www.nndc.bnl.gov/ensdf>.
  - [22] P. Alexa, J. Kvasil, N. V. Minh, and R. K. Sheline, Phys. Rev. C **55**, 179 (1997).
  - [23] T.T.S Kuo, and G.E. Brown, Nucl.Phys. **A85**, 40 (1966).
  - [24] C. Moazed, T.T.S Kuo, and G.E. Brown, Nucl.Phys. **A114**, 241 (1968).
  - [25] C. Moazed, K. Nagatani, and A. Bernstein, Nucl.Phys. **A139**, 1 (1969).
  - [26] L. Coraggio, A. Covello, A. Gargano, and N. Itaco, Phys. Rev. C **73**, 031302(R) (2006).
  - [27] J.A. Fenton, T.H. Kruse, N. Williams, M.E. Williams, R.N. Boyd, W. Savin, Nucl.Phys. **A187**, 123 (1972).
  - [28] D. Rudolph, L.-L. Andersson, R. Bengtsson, J. Ekman, O. Erten, C. Fahlander, E. K. Johansson, I. Ragnarsson, C. Andreoiu, M. A. Bentley, et al., Phys. Rev. C **82**, 054309 (2010).
  - [29] M. Kortelainen, J. Dobaczewski, K. Mizuyama, and J. Toivanen, Phys. Rev. C **77**, 064307 (2008).
  - [30] W. Satula and R. Wyss, Nucl.Phys. **A676**, 120 (2000).
  - [31] E. Chabanat, P. Bonche, P. Haensel, J. Meyer, and R. Schaeffer, Nucl. Phys. **A 635**, 231; 643, 441(E) (1998).
  - [32] J. Bartel, P. Quentin, M. Brack, C. Guet, and H.-B. Håkansson, Nucl.Phys. **A386**, 79 (1982).
  - [33] S.-G. Nilsson and I. Ragnarsson, *Shapes and shells in nuclear structure* (Cambridge university press, Cambridge, 1995).
  - [34] L. Coraggio, A. Covello, A. Gargano, and N. Itaco, Phys. Rev. C **76**, 061303(R) (2007).
  - [35] S. Goriely, N. Chamel, and J. M. Pearson, Phys. Rev. C **88**, 024308 (2013).
  - [36] M. Kortelainen, J. McDonnell, W. Nazarewicz, P.-G. Reinhard, J. Sarich, N. Schunck, M. V. Stoitsov, and S. M. Wild, Phys. Rev. C **85**, 024304 (2012).
  - [37] W. Almosly, B.G. Carlsson, J. Dobaczewski, J. Suhonen, J. Toivanen, P. Vesely and E. Ydrefors, Phys. Rev. C **89**, 024308 (2014).
  - [38] I. Bentley and S. Frauendorf, Phys. Rev. C **88**, 014322 (2013).
  - [39] J. P. Schiffer and W. W. True, Rev. Mod. Phys. **48**, 191 (1976).